CORA Cork Open Research Archive
Cartlann Taighde Oscailte Chorcaí

Title	Impact of gamma irradiation and ethylene oxide sterilisation on the stability of crystalline and amorphous drug solids
Authors	Elkhashab, Mohamed;Sartawi, Ziad;Lynch, Denis;Vucen, Sonja;Crean, Abina
Publication date	2026-06-20
Original Citation	Elkhashab, M, Sartawi, Z, Lynch, D, Vucen, S & Crean, A 2026, 'Impact of gamma irradiation and ethylene oxide sterilisation on the stability of crystalline and amorphous drug solids', European Journal of Pharmaceutical Sciences, vol. 224, 107572, pp. 1-12. https://doi.org/10.1016/j.ejps.2026.107572
Type of publication	Article (peer-reviewed)
Link to publisher's version	https://www.scopus.com/pages/publications/105042227811 - 10.1016/j.ejps.2026.107572
Rights	© 2026, authors. Published by Elsevier B.V. This is an open access article under the CC BY license (http://creativecommons.org/licenses/by/4.0/). - https://creativecommons.org/licenses/by/4.0/
Download date	2026-11-02 00:00:06
Item downloaded from	https://hdl.handle.net/10468/19464



UCC
University College Cork, Ireland
Coláiste na hOllscoile Corcaigh

European Journal of Pharmaceutical Sciences 224 (2026) 107572

Contents lists available at ScienceDirect

European Journal of Pharmaceutical Sciences

journal homepage: www.elsevier.com/locate/ejps

Impact of gamma irradiation and ethylene oxide sterilisation on the stability of crystalline and amorphous drug solids

Mohamed Elkhashab [a], Ziad Sartawi [b], Denis Lynch [c], Sonja Vucen [a], Abina Crean [a,*]

[a] SSPC, The Research Ireland Centre for Pharmaceuticals, School of Pharmacy, University College Cork, Cork, T12 K8AF, Ireland
[b] School of Pharmacy, University College Cork, Cork, T12 K8AF, Ireland
[c] Analytical and Biological Chemistry Research Facility, School of Chemistry, University College Cork, Cork, T12 YN60, Ireland

ARTICLE INFO

Keywords:
Terminal sterilisation
Gamma irradiation
Ethylene oxide
Physicochemical stability
Solid-state characterisation

ABSTRACT

Terminal sterilisation is a critical process for pharmaceutical products intended for parenteral or invasive administration, yet conventional sterilisation approaches can compromise thermolabile or chemically sensitive drug substances. In this study, the compatibility of crystalline and amorphous solid forms of five drug substances (betamethasone dipropionate (BMD), estradiol (E2), itraconazole (ITZ), vismodegib (VDG), and zolmitriptan (ZMT)) with sterilising gamma irradiation and ethylene oxide (EtO) cycles was evaluated in terms of chemical and physical stability. Physical stability was assessed by visual inspection of crystalline powders and amorphous solids pre- and post-sterilisation and by differential scanning calorimetry (DSC) to characterise the melting behaviour of crystalline drugs, and glass transition and recrystallisation events in amorphous forms. Chemical stability was examined using reverse phase-high-performance liquid chromatography (RP-HPLC), liquid chromatography–mass spectrometry (LC-MS), and proton nuclear magnetic resonance spectroscopy (^{1}H-NMR).

Gamma irradiation and EtO preserved the chemical integrity of BMD, E2, ITZ, and VDG. A reversible colour change observed for ITZ was attributed to radical formation as confirmed by gentle heating, HPLC and LC-MS. E2 demonstrated alterations in crystallinity and thermal behaviour after sterilisation, despite maintaining chemical integrity. ZMT exhibited pronounced sensitivity to sterilisation: gamma irradiation induced physical softening and oxidative degradation, particularly in the amorphous form, while EtO sterilisation induced ZMT hydroxyethylation, as confirmed by LC-MS identification of multiple alkylated derivatives.

Overall, sterilisation compatibility was governed primarily by molecular structure rather than the drug solid-state. These findings provide an insight for selecting sterilisation strategies and facilitate the translation of crystalline and amorphous pharmaceutical solids toward clinical application.

1. Introduction

Sterility is a fundamental requirement for pharmaceutical formulations intended for parenteral and invasive routes of administration, as these routes bypass natural protective barriers and therefore demand strict microbiological control to ensure patient safety and product integrity (Hussong, 2010; Tyski et al., 2025). Regulatory authorities such as the European Medicines Agency and the European Pharmacopoeia (Ph. Eur.) define sterilisation as a validated and controlled process capable of achieving a sterility assurance level (SAL) of $\leq 10^{-6}$, acknowledging that absolute sterility can never be guaranteed (Council of Europe, 2019a; "European Medicines Agency," 2019). Consequently, the choice of sterilisation strategy must balance microbial inactivation with preservation of drug quality attributes, including chemical stability, impurity profile, and therapeutic efficacy (Lambert et al., 2011; Speleers et al., 2025; Van Cauwenbergh et al., 2022).

Manufacturing of sterile medicinal products relies on two principal approaches: aseptic processing and terminal sterilisation ("European Medicines Agency," 2019). Terminal sterilisation is generally preferred, as it subjects the product to sterilisation in its final container closure system, thereby minimizing the risk of post-process contamination (Council of Europe, 2019a; Speleers et al., 2025). However, many pharmaceutical compounds and delivery systems are thermolabile or moisture-sensitive, rendering conventional heat- or steam-based sterilisation unsuitable (Li et al., 1998; Pérez Davila et al., 2021; Rediguieri et al., 2016). Under such circumstances, alternative low-temperature

* Corresponding author.
E-mail address: a.crean@ucc.ie (A. Crean).

https://doi.org/10.1016/j.ejps.2026.107572
Received 9 April 2026; Received in revised form 18 May 2026; Accepted 2 June 2026
Available online 6 June 2026
0928-0987/© 2026 The Author(s). Published by Elsevier B.V. This is an open access article under the CC BY license (http://creativecommons.org/licenses/by/4.0/).

sterilisation technologies, particularly ionizing radiation (gamma or electron beam) and ethylene oxide (EtO) gas, are widely applied in both pharmaceutical and medical device industries (Lambert et al., 2011; Van Cauwenbergh et al., 2022).

Gamma irradiation, most commonly generated from cobalt-60 sources (Van Cauwenbergh et al., 2022), offers deep penetration and broad-spectrum antimicrobial activity, making it suitable for terminal sterilisation of packaged products (Harrell et al., 2018; Hasanain et al., 2014; Simmons, 2012). Typical sterilisation doses are around 25 kGy (Aquino and Aquino, 2012; "European Medicines Agency," 2019; Van Cauwenbergh et al., 2022), although higher doses may be applied depending on the bioburden and material compatibility (Nguyen et al., 2006). Numerous studies have demonstrated that gamma irradiation can be successfully applied to a variety of pharmaceutical formulations and drug delivery systems without compromising their structural integrity or therapeutic performance. For example, hydrogel-forming and dissolving microneedle arrays have been shown to retain mechanical strength and drug-release characteristics following gamma sterilisation (Donnelly et al., 2012; McCrudden et al., 2015; Swathi et al., 2020), and polymeric delivery systems such as PLGA microspheres and nanoparticles maintained morphology, drug content, and release kinetics after exposure to sterilisation-relevant doses (Desai et al., 2013; Igartua et al., 2008; Yang et al., 2013).

Despite its effectiveness, gamma irradiation can induce radiolytic degradation of drug molecules through mechanisms such as free radical formation, oxidation, dehalogenation, and cleavage of labile chemical bonds (Jacobs, 2022; Speleers et al., 2025). Gamma irradiation has been shown to induce corticosteroid degradation pathways involving oxidation of the C-11 alcohol group and loss of the C-17 side chain (Bussey et al., 1983; Kane and Tsuji, 1983; Speleers et al., 2025), while dexamethasone has been reported to undergo hydroxyl radical oxidation, radical substitution, and direct molecular decomposition (Guo et al., 2017; Speleers et al., 2025). Antibiotics such as tetracycline have generally shown higher stability in the solid state under irradiation (Boess and Bögl, 1996; Speleers et al., 2025; Van Cauwenbergh et al., 2022), although aqueous solutions were found to be significantly more susceptible to degradation at sterilisation-relevant doses (Boess and Bögl, 1996; Speleers et al., 2025).

EtO sterilisation represents an alternative for products that are incompatible with ionizing radiation or high temperatures. EtO achieves microbial inactivation through alkylation of nucleophilic sites in DNA, RNA, and proteins, thereby disrupting essential cellular processes (Mendes et al., 2012; Van Cauwenbergh et al., 2022). Its effectiveness at relatively low temperatures renders it compatible with a wide range of medical devices and drug-delivery systems, including polymeric implants (Haim Zada et al., 2019; Herczeg and Song, 2022; Tipnis and Burgess, 2018), microneedle arrays (Castilla-Casadiego et al., 2022; Li et al., 2024), and combination products (Lambert et al., 2011; Rutala and Weber, 2023), without significant alteration of their physical structure or performance characteristics.

However, EtO is highly reactive and potentially toxic (Rutala and Weber, 2023), and concerns persist regarding chemical interactions with pharmaceutical compounds as well as the retention of residual EtO and its by-products, such as ethylene chlorohydrin and ethylene glycol (Buben et al., 1999; "ISO 10993-7:2008.; Mendes et al., 2007). Studies have shown that EtO can react with labile hydrogen atoms or nucleophilic functional groups, potentially leading to polymerization, hydrolysis, or formation of adducts in sensitive drug substances (Chen et al., 2015; Hill et al., 2025), including protein therapeutics (Chen et al., 2015). Therefore, stringent control of residual EtO levels and careful assessment of chemical stability after sterilisation are mandatory to ensure patient safety.

Although gamma irradiation and EtO sterilisation are well established for medical devices and combination products, focused investigations into their effects on drug substances remain comparatively limited. Previous work on ophthalmic therapeutics such as dexamethasone, methylprednisolone, acyclovir, tetracycline hydrochloride, and triamcinolone demonstrated that gamma irradiation could lead to the formation of specific impurities in corticosteroids (Speleers et al., 2025; Van Cauwenbergh et al., 2022), while other drugs remained largely compatible with Ph. Eur. requirements under certain irradiation conditions (Krupianskaya et al., 2022; Speleers et al., 2025; Van Cauwenbergh et al., 2022). Beyond conventional crystalline drug substances, the role drug solid-state plays in its response to sterilisation has received less attention. Amorphous and glassy pharmaceutical solids, including melt-quenched glasses and glass-forming drug matrices, have gained increasing importance in advanced drug delivery technologies such as solid dispersions (Leuner and Dressman, 2000), implants (Repka et al., 2012), and microneedle-based systems (Elkhashab et al., 2025; Sartawi et al., 2023). These amorphous systems often exhibit enhanced solubility and bioavailability but are inherently less thermodynamically stable than their crystalline counterparts (Hancock and Zografi, 1997; Yu, 2001), potentially rendering them more vulnerable to radiation- or gas-induced degradation. Despite their growing relevance, systematic studies comparing the sterilisation response of crystalline versus amorphous drug forms are limited.

Therefore, a comprehensive understanding of how terminal sterilisation methods influence both the chemical and physical stability of drug substances is essential for the rational design of sterile drug products and drug delivery systems. In this context, the present work investigates the effects of two clinically relevant terminal sterilisation techniques, gamma irradiation and EtO, on a selection of therapeutic molecules in both crystalline and amorphous (glassy) forms. The selected model compounds, betamethasone dipropionate (BMD), estradiol (E2), itraconazole (ITZ), vismodegib (VDG), and zolmitriptan (ZMT), represent chemically diverse molecules used in dermatological (Charakida et al., 2006), hormonal (Naunton et al., 2006), antifungal (Westerberg and Voyack, 2013), oncological (Sekulic et al., 2012), and neurological therapies (Spencer et al., 1999). By systematically evaluating changes in drug content, impurity profiles, and solid-state properties following sterilisation, this study aims to provide mechanistic insight into sterilisation-induced degradation pathways and to support the development of robust, sterilisation-compatible drug delivery platforms.

2. Materials and methods

2.1. Materials

Vismodegib (VDG) and betamethasone dipropionate (BMD) were purchased from MedChemExpress (Sweden). Itraconazole (ITZ), zolmitriptan (ZMT), and 17-β-estradiol hemihydrate (E2) were supplied by Kemprotec (United Kingdom). Acetonitrile (HPLC gradient grade), water (HPLC gradient grade), methanol (HPLC gradient grade), dimethyl sulfoxide, formic acid, soybean-casein digest medium, fluid thioglycolate medium and triethylamine were obtained from Sigma-Aldrich (Wicklow, Ireland). Parafilm, chromatography vials, and lids were purchased from ThermoFisher Scientific (Ireland). Petri dishes were acquired from Lennox Laboratory Supplies Ltd. (Ireland). T-zero calorimetry pans were sourced from Waters TA Instruments Ireland (Dublin, Ireland).

2.2. Fabrication of amorphous drug forms

Powdered drugs were uniformly spread onto glass slides and placed into a vacuum oven (VACUTHerm, ThermoFisher Scientific, Germany) at temperatures approximately 5°C above their melting temperatures, then cooled to ambient temperature, during which solidification occurred. Details of the melting temperatures and glass transition temperatures (T_g) of each drug are provided in supplementary information (Table S1). The amorphous drug form was confirmed by differential scanning calorimetry (DSC) analysis as described below.

2.3. Sterilisation procedure

Drug powders were sterilised by gamma irradiation and ethylene oxide (EtO) gas sterilisation. All samples were packaged in glass petri dishes sealed with parafilm prior to sterilisation. Gamma sterilisation was conducted at Swann-Morton Limited, United Kingdom. Samples were exposed to a dose of 25 kGy for 10 hours using cobalt 60 tote irradiator. Sterilisation was conducted at room temperature. EtO sterilisation was conducted at Synergy Health Ireland Limited, a STERIS Company, Ireland. Samples were exposed to EtO gas at 50°C and 60% relative humidity for 3 hours, followed by nitrogen washing at 700 mbar and subsequent degassing at 40°C for 8 hours.

2.4. Sterility testing

Sterility of samples was determined following European Pharmacopoeia protocols (Council of Europe, 2019b). Drug powders were directly inoculated into fluid thioglycolate medium (incubated at 32°C) and soybean-casein digest medium (incubated at 22°C) for 14 days. For samples where turbidity was observed after 14 days an additional 5-day incubation in fresh media to confirm microbial growth. Positive controls included *Clostridium sporogenes* for anaerobic conditions and *Staphylococcus aureus* for aerobic conditions, while uninoculated media served as negative controls to verify test validity.

2.5. Physical evaluation post-sterilisation

The visual appearance and thermograms of drug samples pre- and post-sterilisation were compared. DSC analysis was performed using a DSC Q1000 (TA Instruments, UK). Samples were sealed in T-zero calorimetry pans (TA Instruments, Ireland), equilibrated at 25°C for 5 minutes, and heated above their melting points at 3°C/min with a modulation of ±1°C every 60 seconds.

2.6. Chemical evaluation post-sterilisation

Chemical analysis of drugs was performed pre- and post-sterilisation. Proton nuclear magnetic resonance (^{1}H NMR) spectra were acquired at 25°C using a Bruker Avance III spectrometer. Tetramethylsilane was employed as an internal standard for chemical shift calibration, and chemical shifts (δ) were reported in parts per million (ppm), while coupling constants (J) were reported in Hertz (Hz). Spectra for ITZ and BMD were acquired at 600 MHz in deuterated chloroform. VDG and E2 spectra were collected at 400 MHz in deuterated dimethyl sulfoxide, and ZMT spectra were obtained at 600 MHz in deuterated methanol.

Drug quantification was performed by RP-HPLC analysis using an Agilent 1260 Infinity LC system. A Phenomenex Kromasil C8 column was used for ITZ analysis and a Gemini C18 column for other drugs investigated with all columns having dimensions of 250 mm × 4.6 mm and a particle size of 5 μm. An isocratic chromatographic method was used for all drugs. Specific mobile phases and detection wavelengths (λmax) varied per drug as detailed in supplementary information (Table S2). The drug assay was determined from the main drug peak with reference to a calibration curve established for each drug. The percentage recovery was calculated based on the sample mass. Additionally, chromatograms were inspected for any secondary peak indicative of degradation or impurities. The impurity percentage was calculated from the ratio of the impurity peak area to the main drug peak area in the chromatogram.

Liquid Chromatography-Mass Spectrometry (LC-MS) qualitative analyses was conducted to probe chemical stability using a Waters Alliance 2695 system connected to a Waters Micromass Quattro Micro mass spectrometer (ESI+ mode). A reversed-phase Gemini C18 column (250 × 4.6 mm, 5 μm) was used for LC separations, employing consistent MS conditions across drugs: source temperature at 140°C, desolvation at 350°C, nitrogen desolvation flow at 500 L/hr, cone gas flow at 25 L/hr, capillary potential at 3.6 kV, cone potential at 18 V, and m/z scan range 50–1250. The same mobile phases and run times used for the corresponding RP-HPLC methods were applied for LC-MS analysis (Supplementary information, Table S2).

2.7. Statistical analysis

Samples analysed were prepared and measured in triplicate. Statistical analyses were performed using GraphPad Prism 9 (GraphPad Software Inc., USA). RP-HPLC results were compared using one-way analysis of variance (ANOVA). The null hypothesis was that there was no statistically significant difference in drug recovery between the non-sterilised control and sterilised samples. Statistical significance was defined as $p < 0.05$.

3. Results

3.1. Sterility analysis

To assess the effectiveness of both sterilisation techniques, crystalline and amorphous drug samples were assessed post-sterilisation for evidence of microbial growth according to the sterility testing procedure described above. After a 14-day observation period, no bacterial or fungal contamination was detected in any of the drug powders post-sterilisation (Supplementary Information, Figs. S1 to S5). Transient turbidity was observed in crystalline powder samples of ZMT and BMD; therefore, aliquots from these samples were transferred into fresh medium and monitored for a further 5 days. No turbidity or microbial growth was observed indicating effective sterilisation of these samples. The initial turbidity events observed may possibly be attributed to artefacts related to the physicochemical properties of these drug particles.

3.2. Visual observations post-sterilisation

Visual inspection offered insights into potential physical and chemical changes induced by sterilisation. VDG, BMD, and E2 samples displayed no observable changes in morphology or colour following both gamma and ETO sterilisation. However, changes in appearance were noted for ITZ following gamma irradiation (Fig. 1) and ZMT following both gamma and EtO-sterilisation (Fig. 3).

ITZ amorphous sample developed a distinct greyish-green discoloration following gamma irradiation (Fig. 1 f), whereas the crystalline ITZ powder exhibited a noticeable transition to a light brownish colour (Fig. 1 c). The change in appearance may be attributed to macro-radicals generated during exposure to ionizing radiation exposure. Such discoloration was absent in EtO-sterilised ITZ crystalline powder (Fig. 1 b) and amorphous ITZ samples (Fig. 1 e). Similar radical-induced colour centres were previously observed for poly (ethylene terephthalate) (Jamalzadeh et al., 2024), liquid crystal polymers (Houriet et al., 2025) and polycarbonate (Clough et al., 1996). To verify whether the discoloration observed was a transient radical-induced colour change rather than irreversible chemical degradation, the gamma irradiated amorphous samples were heated at 40°C for 5 minutes. Under these conditions, the original colour was restored (Fig. 2), suggesting a reversible radical-induced coloration rather than permanent structural alteration.

An ETO-induced colour change was noted for the ZMT crystalline powder, turning from white to a golden yellow (Fig. 3 b). A comparable amber or golden-yellow colour change was observed in the amorphous ZMT samples immediately after preparation (Fig. 3 d), with no further colour alteration after either sterilisation treatment. However, after both sterilisation methods the amorphous samples exhibited a marked change in morphology, appearing to have lost form due to fusion of particles potentially due to melting during sterilisation. The origin of the colour change observed in the control amorphous samples was examined in the following sections to determine the chemical stability of the ZMT during preparation of the amorphous phase.

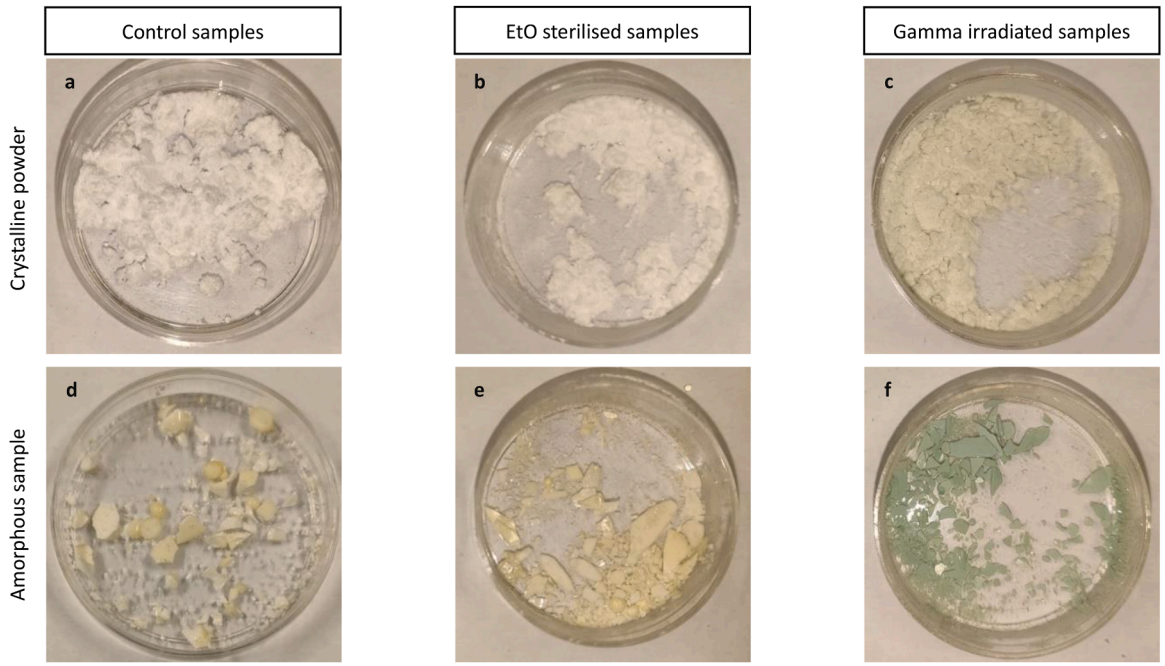


Fig. 1. Itraconazole crystalline and amorphous samples before and after sterilisation process. Crystalline itraconazole samples are shown in panels (a–c): (a) before sterilisation, (b) after ethylene oxide sterilisation, and (c) after gamma irradiation. Amorphous itraconazole samples are shown in panels (d–f): (d) before sterilisation, (e) after ethylene oxide sterilisation, and (f) after gamma irradiation.



Fig. 2. (a) Itraconazole amorphous sample before sterilisation; (b) Gamma irradiated itraconazole amorphous sample; (c) the same sample after heating at 40°C for 5 minutes demonstrating reversal of the irradiation-induced colour change.

3.3. Drug solid-state form post-sterilisation

DSC analysis was conducted to evaluate drug solid-state stability post-sterilisation. DSC thermograms of sterilised crystalline ITZ, VDG, BMD, and E2 showed clearly defined melting endotherms consistent with their previously reported melting temperatures detailed in supplementary information (Table S1). Temperatures were observed post-gamma irradiation and EtO sterilisation (Fig. 4 a-d) indicating no significant sterilisation-induced change in melting behaviour. Amorphous ITZ, VDG, and BMD samples displayed similar DSC thermograms pre- and post-sterilisation, indicating that sterilisation did not alter their thermal behaviour (Fig. 5 a-c). Thermograms displayed typical behaviour of amorphous drug forms; a characteristic T_g, followed by an exothermic crystallisation event, and a subsequent endothermic melt. T_g values observed were also similar to previously reported values detailed in supplementary information (Table S1).

Of note was an increase in the crystallisation exotherm temperature for amorphous ITZ post-sterilisation. The crystallisation peak of the non-sterilised amorphous ITZ control was observed at 120.1 ± 0.8°C, while gamma-irradiated and EtO-sterilised amorphous ITZ showed crystallisation peaks at 125.4 ± 0.9°C and 121.89 ± 0.9°C, respectively (Fig. 5 a). This shift was significant post-gamma irradiation ($p < 0.05$). Similar changes in cool crystallisation-related DSC events have previously been reported after gamma irradiation in amorphous and semicrystalline materials, which were attributed to irradiation-induced changes in material structure, crystallinity, or molecular mobility (Marcos Rios et al., 2026; Milicevic et al., 2007)

The amorphous stability of E2 was undermined by both gamma irradiation and EtO sterilisation. DSC thermograms displayed a reduced enthalpy of crystallisation following both gamma irradiation and EtO sterilisation of the amorphous samples (Fig. 5 d). The enthalpy of crystallisation (ΔH_c) was determined to be 14.16 J/g for the gamma irradiated sample and 5.72 J/g for the EtO-sterilised sample, in contrast to 34 J/g for the amorphous E2 sample pre-sterilisation. To further investigate differences in crystalline content, a degree of crystallinity parameter was estimated using equation 1, adapted for an equation originally developed to determine the degree of crystallinity in polymeric films (Murthy et al., 1994),

$$X_c = \frac{\Delta H_m - \Delta H_c}{\Delta H_{ref}} \quad (1)$$

where X_c is the degree of crystallinity ΔH_m is the enthalpy of the melting

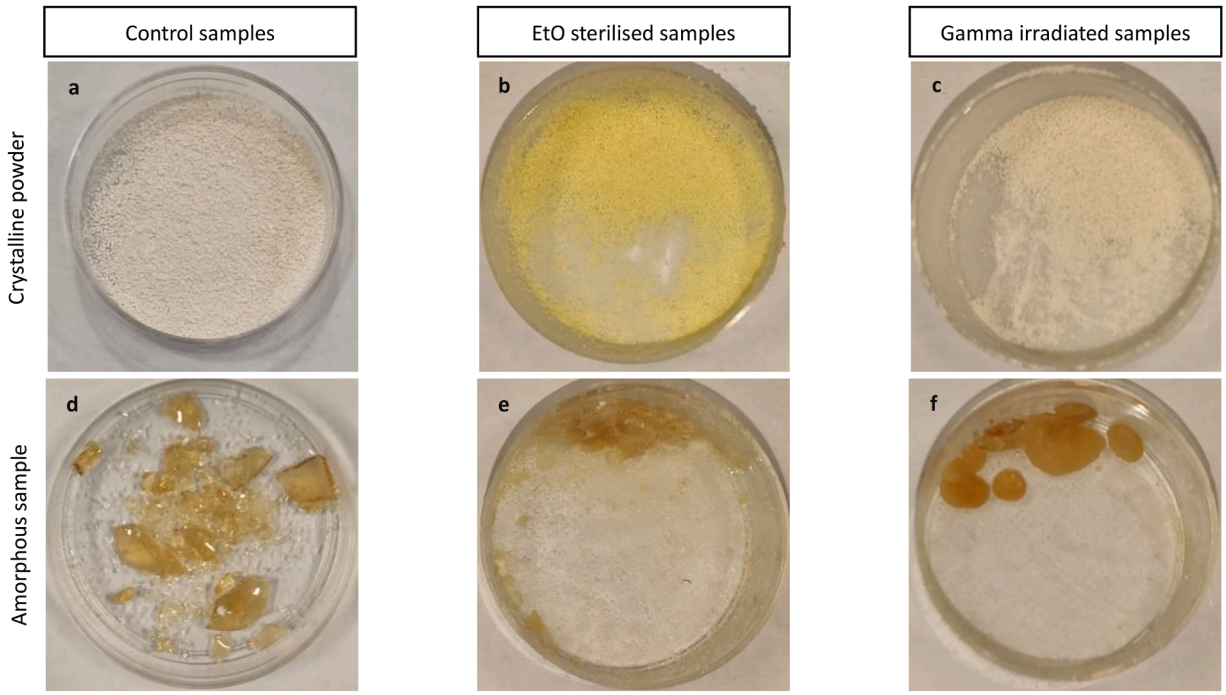


Fig. 3. Zolmitriptan crystalline and amorphous samples before and after sterilisation process. Crystalline zolmitriptan samples are shown in panels (a–c): (a) before sterilisation, (b) after ethylene oxide sterilisation, and (c) after gamma irradiation. Amorphous zolmitriptan samples are shown in panels (d–f): (d) before sterilisation, (e) after ethylene oxide sterilisation, and (f) after gamma irradiation.

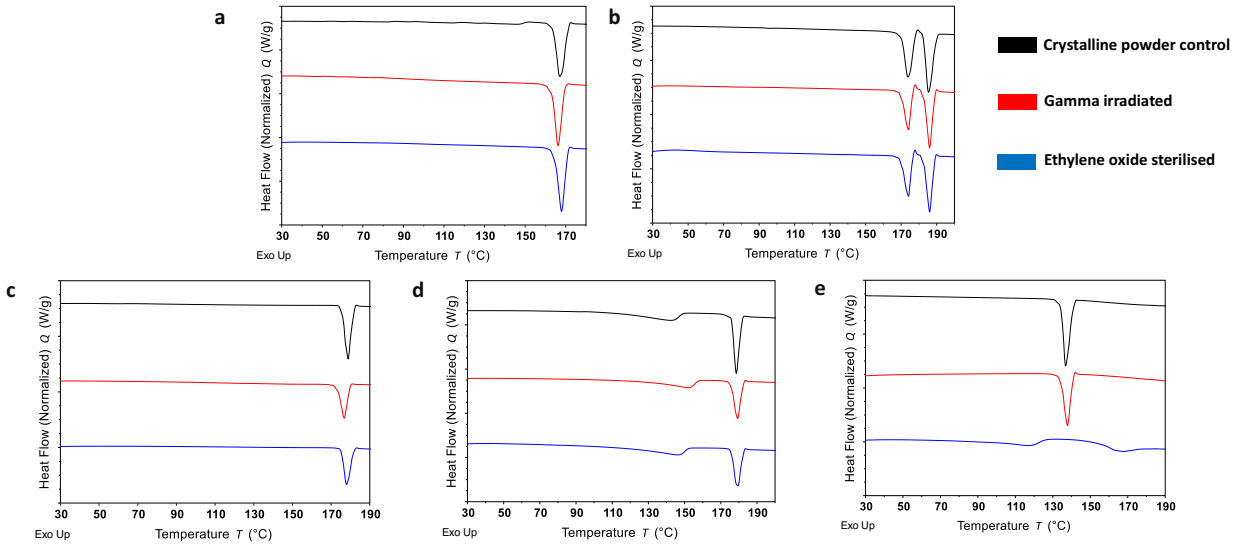


Fig. 4. Representative DSC thermogram of crystalline powder of (a) itraconazole, (b) vismodegib, (c) betamethasone dipropionate, (d) estradiol, and (e) zolmitriptan pre and post gamma irradiation and ethylene oxide sterilisation.

peak, ΔH_c is the enthalpy of the crystallisation peak, and ΔH_{ref} is the enthalpy of the melting peak of the control crystalline sample. Using this approach, the calculated degree of crystallinity of gamma-irradiated amorphous E2 sample was determined to be 0.78, while that of the EtO sterilised amorphous E2 sample was 0.87, both considerably higher than the amorphous form pre-sterilisation (0.48).

Of the drugs investigated, ZMT displayed the greatest changes in solid-state form post-sterilisation. The crystalline ZMT sample before sterilisation displayed a clear endothermic melting peak at 136°C, the reported melting point of zolmitriptan (Ravikumar et al., 2007). Post-EtO sterilisation, the endothermic melting peak at 136°C was not evident, indicating a loss of solid-state form. In contrast, ZMT crystalline solid-state form appeared to be unaffected by gamma-irradiation. Post-gamma-irradiation, thermograms of crystalline ZMT displayed a sharp endothermic melting peak at 136°C (Fig. 4 e), in agreement with the thermogram for crystalline ZMT pre-sterilisation. Amorphous ZMT post-gamma irradiation exhibited a reduced T_g of 19°C compared to the pre-sterilised control of 49°C (Fig. 5 e), indicating plasticisation of the amorphous phase. The thermogram of amorphous ZMT post-EtO sterilisation displayed a melting transition at 136°C but with no observable preceding T_g or crystallisation event (Fig. 5 e). This behaviour indicates recrystallisation and a loss of amorphous content, suggesting that exposure to the EtO sterilisation conditions (3 hours at 50°C, 60% relative humidity) may compromise the amorphous stability of the

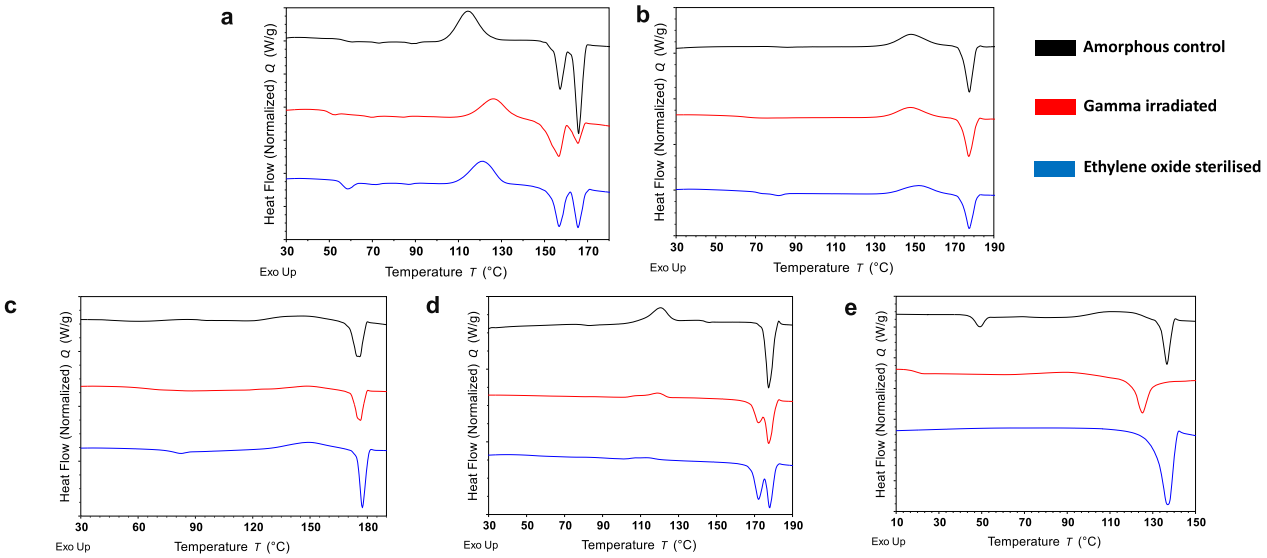


Fig. 5. Representative DSC thermogram of amorphous samples of (a) itraconazole, (b) vismodegib, (c) betamethasone dipropionate, (d) estradiol, and (e) zolmitriptan pre- and post-gamma irradiation and ethylene oxide sterilisation.

sample.

3.4. Chemical stability assessment by RP-HPLC and LC-MS

To probe sterilisation-induced chemical instability and elucidate associated chemical degradation products, drug samples were analysed by RP-HPLC and LC-MS pre- and post-sterilisation. For all drugs, except for ZMT, RP-HPLC analysis revealed no significant reduction in the drug assay post-sterilisation using one-way ANOVA analysis ($p > 0.05$), irrespective of drug solid-state (crystalline or amorphous) or sterilisation method (gamma irradiation or EtO) (Fig. 6). BMD and VDG exhibited assay values within ± 2% of the nominal values, indicating minimal or no sterilisation-induced chemical degradation. This result was confirmed by LC-MS analysis (Supplemental Information, Figs. S6 and S7). LC-MS analysis of ITZ samples post-gamma irradiation identified the presence of a degradation product with a mass of 671.27 g/mol (Fig. 7), which was previously reported (Dettlaff et al., 2014; Sartawi et al., 2023). The amount of this impurity remained minimal; 0.29 ±0.01% in samples of crystalline ITZ and 0.23±0.01% in amorphous ITZ post-sterilisation.

E2 assay consistently ranged from 98.89% to 99.92% following both sterilisation procedures. LC-MS analysis of E2 revealed no detectable structural modifications or additional peaks post-sterilisation (Supplemental Information, Fig. S8), further affirming its chemical stability.

In contrast, RP-HPLC analysis of ZMT demonstrated significant chemical instability post sterilisation, particularly after EtO sterilisation of its crystalline form (Fig. 6 e). Analysis revealed a reduction in ZMT assay, with levels falling to approximately 61%. This decline was accompanied by the appearance of several new chromatographic peaks at retention times of 2.29, 4.77, 5.16, 5.90, 6.56, and 6.94 minutes, indicative of the formation of multiple degradation products (Fig. 8 a).

To investigate the degradation products of ZMT following EtO sterilisation, proposed EtO-induced reaction products were developed, with corresponding molecular masses summarised in Table 1. These theoretical degradation products were then assessed for their presence in the LC-MS data. An electrospray ionization in positive mode (ES^+) scan was conducted to confirm the presence of these predicted species. The ES^+ scan revealed specific chemical transformations attributable to EtO sterilisation. A major degradation product was observed at a mass-to-charge ratio (m/z) of 376.2, corresponding to the addition of two ethylene oxide units (+88 Da relative to native ZMT), suggesting nucleophilic alkylation reactions. Another prominent product was detected at m/z 420.2, representing the addition of three ethylene oxide units (+132 Da relative to ZMT). Additionally, a notable species at m/z

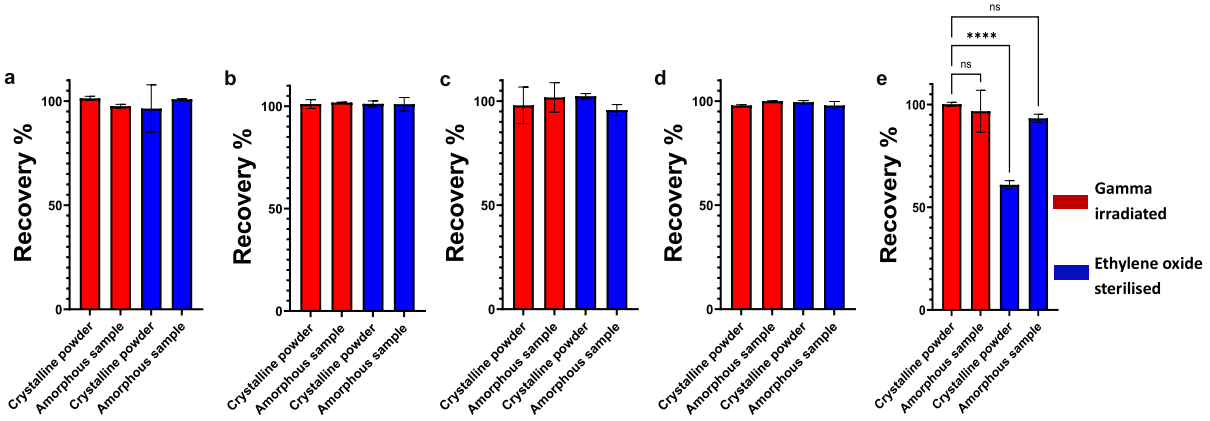


Fig. 6. HPLC analysis of drug recovery after gamma irradiation and ethylene oxide sterilisation of both the crystalline powder and amorphous samples of (a) itraconazole; (b) vismodegib; (c) betamethasone dipropionate; (d) estradiol; and (e) zolmitriptan.

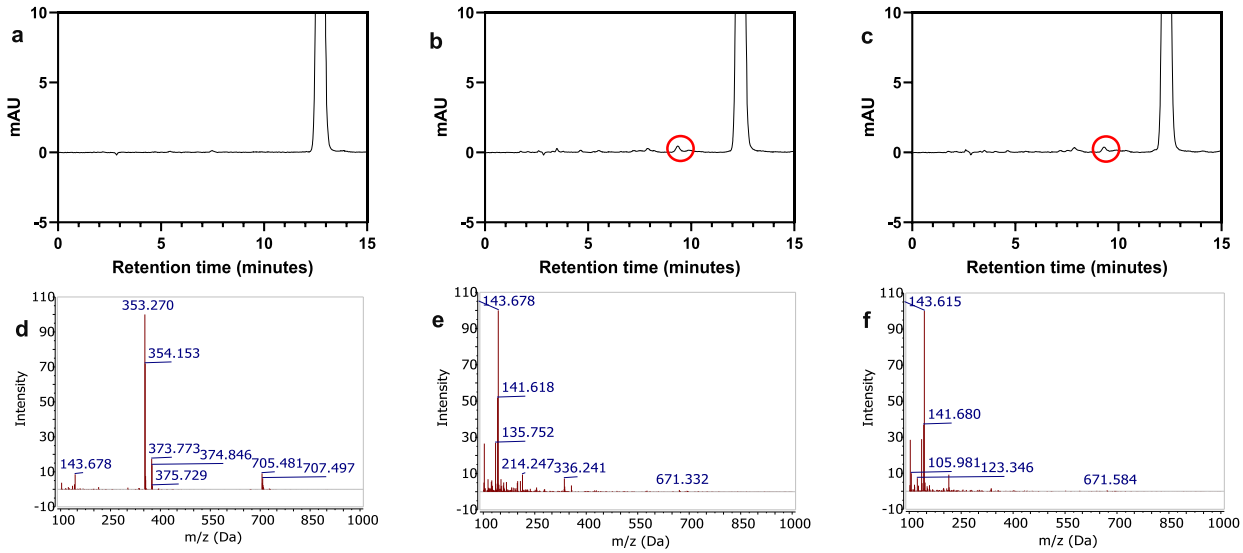


Fig. 7. Representative UV chromatograms and LC-MS spectra of itraconazole control and gamma irradiated crystalline and amorphous samples, zoomed in to focus on regions highlighting sample degradation. (a-c) UV chromatogram of (a) control Itraconazole, (b) gamma irradiated crystalline itraconazole, and (c) gamma irradiated amorphous itraconazole. The degradation product peak detected after gamma irradiation is highlighted with a red circle. (d-f) LC-MS spectra of (d) itraconazole main peak, (e) gamma irradiated crystalline itraconazole, and (f) gamma irradiated amorphous itraconazole. The corresponding impurity had a molecular weight of 671.27 g/mol based on LC-MS analysis.

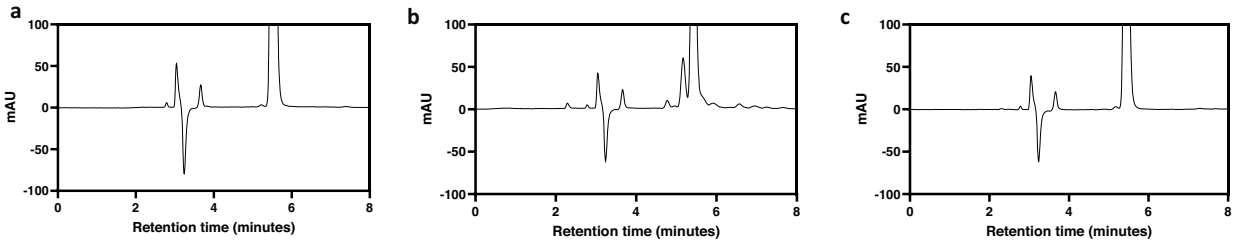


Fig. 8. Representative UV chromatogram of zolmitriptan before and after ethylene oxide sterilisation, zoomed in to focus on regions highlighting sample degradation. (a) unsterilised zolmitriptan control sample, (b) sterilised zolmitriptan crystalline powder, and (c) sterilised zolmitriptan amorphous sample.

332.2 was consistent with zolmitriptan modified by a single hydroxyethyl substitution. A further degradation product, detected at m/z 303.2, suggested oxidative modification of the indole moiety, highlighting extensive structural disruption following EtO sterilisation (Supplemental information, Figs. S10 and S11).

Prior to investigating the effect of sterilisation on the stability of the amorphous ZMT sample, the impact of amorphous form generation on its stability was investigated due to the amber or golden-yellow colour change was observed in the amorphous ZMT samples immediately after preparation (Fig. 3 d). The RP-HPLC analysis showed no significant difference, and the ES^+ scan of the pre-sterilised amorphous form of ZMT showed no detectable change compared to that of the crystalline control (Supplemental Information, Fig. S9 and Fig. S13). These results indicate that the colour change observed after preparation is a characteristic of the physical form of ZMT rather than an indication of chemical degradation.

Interestingly, when the amorphous sample of ZMT was subjected to EtO sterilisation, RP-HPLC assay was substantially higher, at approximately 93% (Fig. 6 e). Only a minor additional chromatographic peak at 5.17 minutes was detected (Fig. 8 b), indicating markedly reduced chemical reactivity compared to the crystalline powder. LC-MS analysis revealed the same degradation products in the amorphous sample as those observed in the crystalline powder (Supplemental Information, Fig. S11), suggesting that the reduced degradation may be primarily due to a decreased surface area of exposure rather than an inherent improvement in the chemical stability of the amorphous sample.

In comparison, gamma irradiation induced fewer chemical changes in ZMT. LC-MS analysis of gamma-irradiated ZMT amorphous sample revealed minor low-mass fragment ions at m/z 304 (Supplemental Information, Fig. S12), indicative of indole oxidation and similar to the degradation observed with EtO treatment. This oxidative damage likely contributed to the yellow discoloration and morphological changes, observed in the amorphous samples following gamma irradiation. However, the gamma-treated samples showed no evidence of the extensive chemical modifications or mass additions typically associated with EtO sterilisation, underscoring the distinct mechanisms of chemical alteration underlying each sterilisation method.

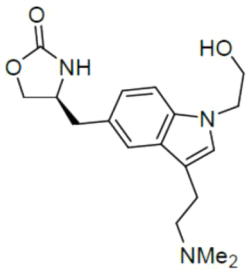
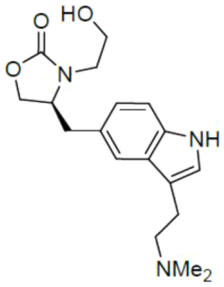
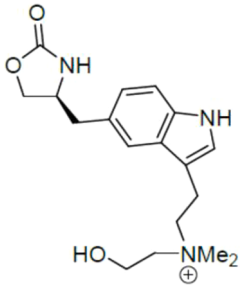
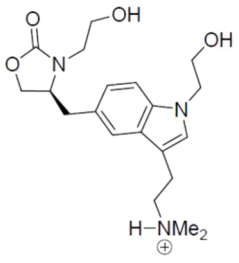
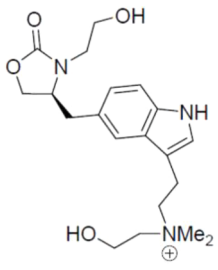
3.5. *Nuclear magnetic resonance spectroscopy (NMR) analysis*

^{1}H NMR spectroscopy further confirmed the structural stability profiles obtained from RP-HPLC and LC-MS analyses. The sterilised samples of ITZ, BMD, VDG, and E2 exhibited NMR spectra indistinguishable from their non-sterilised counterparts, reinforcing the absence of structural modifications across both sterilisation methods and physical states (Supplementary Information, Figs. S14 and S15). In contrast, ZMT demonstrated pronounced NMR spectral changes following EtO sterilisation of its crystalline form. ^{1}H NMR spectroscopy of the treated samples correlated well with the results of LC-MS analysis, supporting identification of hydroxyethyl-substituted ZMT derivatives as impurities.

The crystalline form of ZMT showed significant evidence of impurity

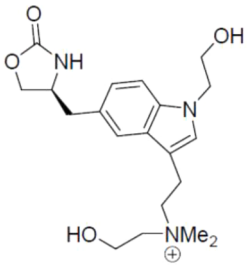
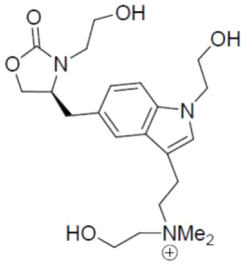
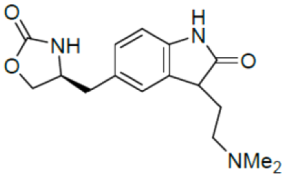
formation post-EtO sterilisation. Spectral features consistent with alkylation of ZMT, via ring-opening of ethylene oxide, were observed in the ^{1}H NMR spectra of the treated material. Resonances not associated with ZMT were seen in the aliphatic regions 3.10–3.40 ppm and 3.50–3.90 ppm, along with broad singlets at 3.98 ppm and 4.06 ppm and resonances overlapping with the ZMT multiplet signal at 4.12–4.25 ppm; these signals are all consistent with the NCH_2 and CH_2OH hydrogens that would result from N-alkylation reaction of ZMT with ethylene oxide at one or more of its three nitrogens (Fig. 9). The more upfield additional signals (3.10–3.40 ppm) can be expected to correspond to NCH_2 hydrogens, while the more downfield additional signals (over the range 3.50–4.25 ppm) are expected to correspond to CH_2OH hydrogens.

Table 1
Proposed structure and identified degradation products of zolmitriptan following ethylene oxide sterilisation, detected by positive mode electrospray ionization mass spectrometry.

Chemical degradation	Proposed structure	Chemical formula	Molecular mass (Da)
Alkylation with single hydroxyethyl substitution		$C_{18}H_{25}N_3O_3$	331.18959
		$C_{18}H_{25}N_3O_3$	331.18959
		$C_{18}H_{26}N_3O_3^+$	332.19687
Alkylation with two hydroxyethyl substitution		$C_{20}H_{30}N_3O_4^+$	376.22308
		$C_{20}H_{30}N_3O_4^+$	376.22308

(continued on next page)

Table 1 (*continued*)

Chemical degradation	Proposed structure	Chemical formula	Molecular mass (Da)
		$C_{20}H_{30}N_3O_4^+$	376.22308
Alkylation with three hydroxyethyl substitution		$C_{22}H_{34}N_3O_5^+$	420.24930
Indole oxidation		$C_{16}H_{21}N_3O_3$	303.15829

The aromatic region shows further impurity signals, perhaps most prominently at 7.22 ppm and 7.36 ppm, that indicate modification at the indole ring. These may be the result of oxidation of the indole moiety or alkylation of the indole nitrogen.

Comparison of the ^{1}H NMR spectra of the ZMT crystalline control and pre-sterilised amorphous showed no detectable spectral changes, further supporting the LC-MS observations described above and the hypothesis that the ZMT colour change observed after preparation is a characteristic of the physical form rather han an indication of chemical degradation. Close examination of the ^{1}H NMR spectrum of amorphous form of ZMT, post treatment in the presence of EtO, revealed signals similar to, or matching, those the observed for the crystalline form of ZMT, albeit at a much lower level (Fig. 10). These features were more clearly seen in the aliphatic region than in the aromatic region.

4. Discussion

This study systematically evaluated the impact of two clinically relevant terminal sterilisation methods gamma irradiation and EtO sterilisation on both crystalline and amorphous forms of five drug substances: BMD, E2, ITZ, VDG, and ZMT. While both sterilisation methods achieved SALs compliant with Ph. Eur. requirements, the physicochemical response of the drug substances investigated was dependent on their molecular structure and in some cases the solid-state form. These findings reinforce the concept that sterilisation compatibility cannot be generalized across drug classes and must be evaluated on a compound-specific basis.

Gamma irradiation at 25 kGy preserved the chemical integrity of four of the five model drugs investigated. BMD and VDG showed no significant changes in thermal behaviour or molecular structure confirming their compatibility with ionizing radiation under the applied

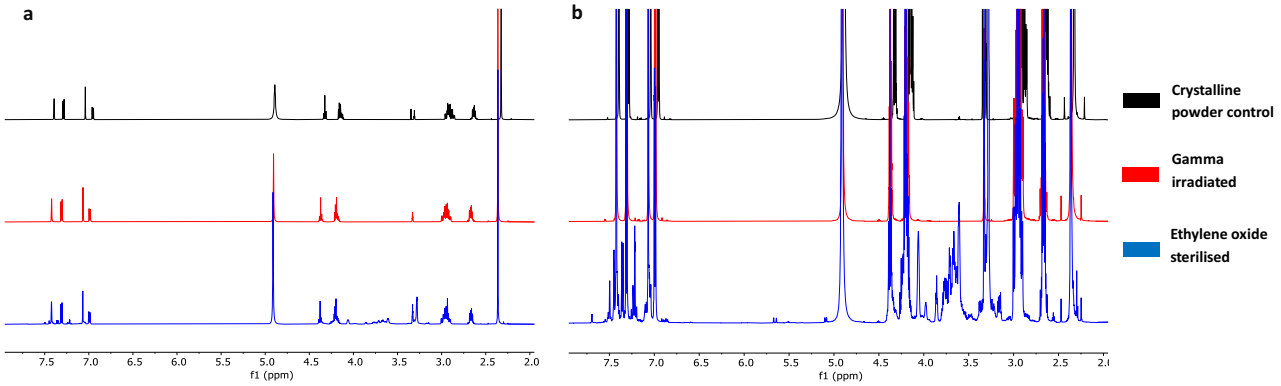


Fig. 9. Representative ^{1}H-NMR spectrum of crystalline powders of (a) zolmitriptan and (b) zoomed zolmitriptan post gamma irradiation and ethylene oxide sterilisation.

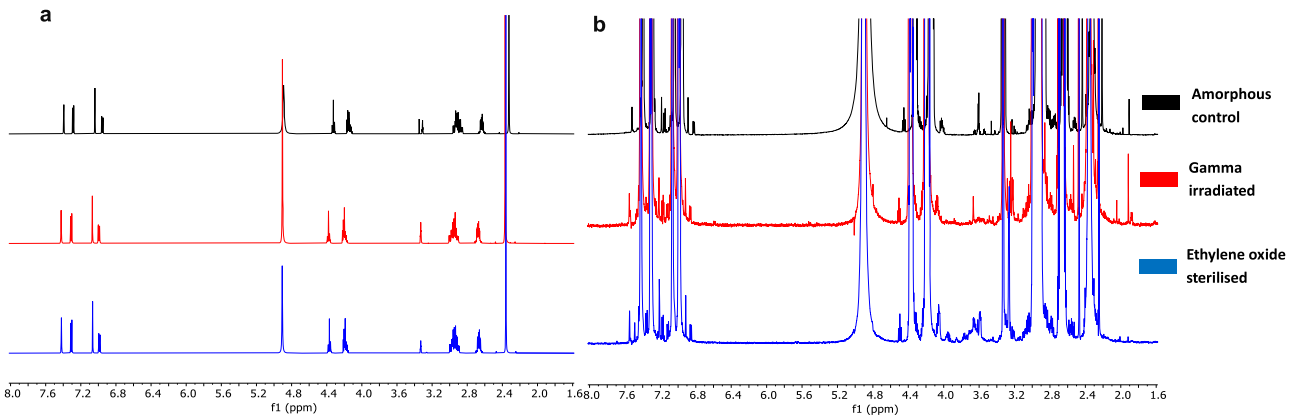


Fig. 10. Representative ^{1}H-NMR spectrum of amorphous samples of (a) zolmitriptan and (b) zoomed zolmitriptan post gamma irradiation and ethylene oxide sterilisation.

conditions. ITZ exhibited a distinct but non-destructive response to gamma irradiation, characterized by a reversible greyish–green discolouration that was more pronounced in the amorphous form. The disappearance of this discolouration after mild thermal treatment indicates that the phenomenon was optical rather than chemical in nature. Similar irradiation-induced colour changes in ITZ have also been reported previously (Dettlaff et al., 2014; Sartawi et al., 2023). Such reversible colour changes have previously been described in polymers and attributed to the formation of annealable colour centres due to transient alterations in molecular structure that affect light absorption but are not chemically destructive (Jamalzadeh et al., 2024). The metastable glassy state of amorphous ITZ, which has been described as exhibiting liquid-crystalline characteristics (Elkhashab et al., 2025; Kozyra et al., 2018), may facilitate the temporary trapping of radiation-induced radicals within the molecular matrix. Similar phenomena have been reported with other compounds, such as sulfamethoxazole (Ogrodowczyk et al., 2011) and cyclophosphamide (Varshney and Dodke, 2004), where radiation exposure resulted in temporary colour changes linked to radical-induced shifts in colour properties rather than molecular degradation. A minor impurity was observed in both the crystalline and amorphous forms of ITZ, with RP-HPLC and LC-MS detecting a low-level radiolytic impurity (~0.27%), consistent with previously reported dehalogenation (Cl) products resulting from gamma irradiation (Dettlaff et al., 2014; Sartawi et al., 2023). However, this impurity was present in comparable amounts in both solid-state forms and does not fully account for the colour disparity between them. The absence of new peaks in the HPLC and NMR spectra, together with only trace radiolytic impurities detected by LC–MS, confirms that no permanent chemical degradation occurred for ITZ.

In contrast, E2 displayed altered solid-state behaviour following both gamma irradiation and EtO sterilisation. Although RP-HPLC assay values remained high and no structural changes were detected by ^{1}H-NMR spectroscopy, DSC analysis revealed a loss in amorphous content and drug recrystallisation. These findings suggest that sterilisation primarily affected the supramolecular structure of E2 rather than its chemical structure. This observation aligns with previous studies showing that certain corticosteroids and 17β-estradiol drug substances can tolerate sterilisation doses of gamma irradiation under controlled conditions (Bussey et al., 1983; Mohr et al., 1999), although radiolytic impurities and solid-state modifications have been described for certain formulations under specific processing parameters (Speleers et al., 2025).

BMD, ITZ, and VDG were compatible with EtO sterilisation as shown by the preservation of thermal properties and molecular integrity. For gamma-irradiated amorphous ITZ, an increase in crystallisation peak temperature was observed. The increase in crystallisation temperature of the ITZ samples post-sterilisation indicates that sample gamma sterilisation enhanced the stability of the amorphous ITZ sample, and this may relate to a reduction in molecular mobility following irradiation. However, more in-depth analysis is required to elucidate the effect of the sterilisation process on the ITZ amorphous sample's cold crystallisation behaviour. It should be noted that the absence of experimental controls to account for the effect of sample storage and time on the sample cold crystallisation behaviour limits the ability to relate this change in crystallisation temperature to solely gamma-irradiation in this study.

ZMT demonstrated pronounced chemical sensitivity to EtO exposure. LC–MS analysis revealed the formation of multiple alkylation products consistent with hydroxyethylation reactions, indicating direct chemical modification of its molecular structure. ZMT contains several labile hydrogen atoms associated with nitrogen functionalities, which are known targets for EtO-mediated alkylation. The detection of products bearing up to three hydroxyethyl substitutions confirms that EtO-induced chemical reactions can occur even under standard EtO sterilisation conditions. LC–MS spectra demonstrated that both ZMT solid forms produced identical degradation products. However, RP-HPLC analysis determined a higher recovery for amorphous ZMT following EtO sterilisation compared to the crystalline form, indicating less degradation. The lower level of degradation observed for the amorphous ZMT was further evidenced by NMR analysis. The ^{1}H NMR spectrum of amorphous ZMT, post-EtO sterilisation revealed similar signals but at a much lower level than its crystalline form counterpart. The reduced degradation may be explained by the reduced surface area:mass ratio of the amorphous ZMT sample compared to the crystalline. The lower surface area would limit EtO penetration, thereby decreasing chemical modification without eliminating chemical reactivity.

VDG showed no evidence of EtO-induced alkylation or structural modification, which can be attributed to the presence of chemically stable functional groups such as a tertiary amide. The amide nitrogen is strongly resonance-stabilized and therefore weakly nucleophilic (Bao et al., 2021; Kaiser et al., 2018), which likely reduces susceptibility to EtO-mediated alkylation under the conditions studied.

These findings revealed that, in assessing the compatibility of crystalline and amorphous drug forms with two sterilisation processes, the solid-state structure plays an important but secondary role relative to molecular structure. The amorphous form of ZMT exhibited greater physical softening and oxidative degradation than its crystalline counterpart following gamma irradiation, consistent with its higher molecular mobility and elevated free energy state (Vranić, 2004). In contrast, amorphous ITZ showed only reversible optical effects with no evidence of permanent chemical degradation. E2 displayed an intermediate behaviour, in which sterilisation induced measurable changes in crystallinity and thermal properties without detectable chemical modification. These contrasting outcomes demonstrate that, although

amorphous systems may be more vulnerable to sterilisation stress in some cases, this effect is not universal and depends strongly on chemical composition.

Overall, this work demonstrates that terminal sterilisation of crystalline and amorphous drug substances is viable but needs to be assessed on a case-by-case basis. Gamma irradiation proved broadly compatible with most of the drugs studied, with only reversible optical effects observed for ITZ and E2 recrystallisation. EtO sterilisation was likewise suitable for several compounds but induced chemical modification in ZMT due to its reactive functional groups. These results provide insight into the relationship between molecular structure, solid-state form, and sterilisation response and provide a scientific basis for supporting terminal sterilisation strategies for both crystalline and amorphous pharmaceutical solids, thereby supporting their future clinical translation.

5. Conclusion

This work provides a systematic assessment of the chemical and physical compatibility of crystalline and amorphous forms of five drug molecules with gamma irradiation and ethylene oxide sterilisation. While both sterilisation methods achieved the required SAL, their influence on physicochemical stability varied markedly according to their molecular structure and, to a lesser extent, physical form. Gamma irradiation maintained the chemical and physical integrity of BMD, ITZ, and VDG with only minor reversible chemical effects on ITZ. While E2 was shown to be chemically compatible with both sterilisation techniques, E2 amorphous stability was undermined by both techniques, with the increased crystalline content detected. ZMT exhibited chemical reactivity combined with physical instability upon exposure to both sterilisation techniques. ZMT hydroxyethylation upon exposure to EtO was elucidated for both crystalline and amorphous forms. Gamma irradiation sterilisation induced ZMT melting and oxidative changes. These findings highlight the need for molecule-specific evaluation of drug molecule compatibility with specific sterilisation procedures. Collectively, these findings demonstrate that terminal sterilisation of drug solid forms by gamma irradiation and EtO sterilisation must be guided by drug chemical functionality and its susceptibility to radiation- or alkylation-mediated reactions, respectively.

CRediT authorship contribution statement

Mohamed Elkhashab: Writing – review & editing, Writing – original draft, Visualization, Validation, Software, Methodology, Investigation, Formal analysis, Data curation, Conceptualization. **Ziad Sartawi:** Software, Methodology, Formal analysis, Data curation. **Denis Lynch:** Writing – original draft, Formal analysis. **Sonja Vucen:** Writing – review & editing, Supervision. **Abina Crean:** Writing – review & editing, Validation, Supervision, Software, Resources, Project administration, Funding acquisition, Conceptualization.

Declaration of competing interest

The authors declare that they have no known competing financial interests or personal relationships that could have appeared to influence the work reported in this paper

Acknowledgements

This publication has emanated from research conducted with the financial support of Taighde ´Eireann – Research Ireland, under Grant number [12/RC/2275(P2)].

Supplementary materials

Supplementary material associated with this article can be found, in the online version, at doi:10.1016/j.ejps.2026.107572.

Data availability

Data will be made available on request.

References

Aquino, K.A., da, S., Aquino, K.A., da, S., 2012. Sterilization by Gamma Irradiation. Gamma Radiation. https://doi.org/10.5772/34901.

Bao, C.C., Du, H.Z., Luo, Y.L., Guan, B.T., 2021. Direct alkylation of N,N-dialkyl benzamides with methyl sulfides under transition metal-free conditions. Commun. Chem. 1 (4), 138-. https://doi.org/10.1038/s42004-021-00575-2, 2021 4.

Boess, C., Bögl, K.W., 1996. Influence of radiation treatment on pharmaceuticals - a review: Alkaloids, morphine derivatives, and antibiotics. Drug Dev. Ind. Pharm. 22, 495–529. https://doi.org/10.3109/03639049609108354;REQUESTEDJOURNAL:JOURNAL:IDDI20.

Buben, I., Melicherčíková, V., Novotná, N., Svitáková, R., 1999. Problems associated with sterilization using ethylene oxide. Residues in treated materials. Cent. Eur. J. Public Health 7, 197–202.

Bussey, D.M., Kane, M.P., Tsuji, K., 1983. Sterilization of Corticosteroids by 60Co Irradiation. PDA J. Pharm. Sci. Technol. 37.

Castilla-Casadiego, D.A., Miranda-Muñõz, K.A., Roberts, J.L., Crowell, A.D., Gonzalez-Nino, D., Choudhury, D., Aparicio-Solis, F.O., Servoss, S.L., Rosales, A.M., Prinz, G., Zou, M., Zhang, Y., Coetzee, J.F., Greenlee, L.F., Powell, J., Almodovar, J., 2022. Biodegradable microneedle patch for delivery of meloxicam for managing pain in cattle. PLoS One 17, e0272169. https://doi.org/10.1371/JOURNAL.PONE.0272169.

Charakida, A., Dadzie, O., Teixeira, F., Charakida, M., Evangelou, G., Chu, A.C., 2006. Calcipotriol/betamethasone dipropionate for the treatment of psoriasis. Expert Opin. Pharmacother. 7, 597–606. https://doi.org/10.1517/14656566.7.5.597.

Chen, L., Sloey, C., Zhang, Z., Bondarenko, P.V., Kim, H., Ren, D., Kanapuram, S., 2015. Chemical modifications of therapeutic proteins induced by residual ethylene oxide. J. Pharm. Sci. 104, 731–739. https://doi.org/10.1002/jps.24257.

Clough, R.L., Gillen, K.T., Malone, G.M., Wallace, J.S., 1996. Color formation in irradiated polymers. Rad. Phys. Chem. 48, 583–594. https://doi.org/10.1016/0969-806X(96)00075-8.

Council of Europe, 2019a. European Pharmacopoeia: methods of preparation of sterile products, 10th ed. Strasbourg, France.

Council of Europe, 2019b. European Pharmacopoeia: Sterility, Chapter 2.6.1, 10th ed. Strasbourg, France.

Desai, K.G.H., Kadous, S., Schwendeman, S.P., 2013. Gamma irradiation of active self-healing PLGA microspheres for efficient aqueous encapsulation of vaccine antigens. Pharm. Res. 30, 1768–1778. https://doi.org/10.1007/S11095-013-1019-2.

Dettlaff, K., Talik, P., Spólnik, G., Danikiewicz, W., Ogrodowczyk, M., 2014. The Influence of Ionizing Radiation on Itraconazole in the Solid State. AAPS Pharm.Sci. Tech. 16, 21–29. https://doi.org/10.1208/S12249-014-0185-9/FIGURES/10.

Donnelly, R.F., Singh, T.R.R., Garland, M.J., Migalska, K., Majithiya, R., McCrudden, C. M., Kole, P.L., Mahmood, T.M.T., McCarthy, H.O., Woolfson, A.D., 2012. Hydrogel-forming microneedle arrays for enhanced transdermal drug delivery. Adv. Funct. Mater. 22, 4879–4890. https://doi.org/10.1002/ADFM.201200864.

Elkhashab, M., Sartawi, Z., Faisal, W., Crean, A., 2025. Glassy drug microneedle array design: drug glass-forming ability and stability. Mol. Pharm. 22, 1373–1383. https://doi.org/10.1021/ACS.MOLPHARMACEUT.4C01067/ASSET/IMAGES/LARGE/MP4C01067_0010.JPEG.

European Medicines Agency [WWW Document], 2019. URL. https://www.ema.europa.eu/en/sterilisation-medicinal-product-active-substance-excipient-primary-container-scientific-guideline. accessed 3.30.26.

Guo, Z., Guo, A., Guo, Q., Rui, M., Zhao, Y., Zhang, H., Zhu, S., 2017. Decomposition of dexamethasone by gamma irradiation: Kinetics, degradation mechanisms and impact on algae growth. Chem. Eng. J. 307, 722–728. https://doi.org/10.1016/J.CEJ.2016.08.138.

Haim Zada, M., Kumar, A., Elmalak, O., Mechrez, G., Domb, A.J., 2019. Effect of Ethylene Oxide and Gamma (γ-) Sterilization on the Properties of a PLCL Polymer Material in Balloon Implants. ACS Omega 4, 21319–21326. https://doi.org/10.1021/ACSOMEGA.9B02889.

Hancock, B.C., Zografi, G., 1997. Characteristics and significance of the amorphous state in pharmaceutical systems. J. Pharm. Sci. 86, 1–12. https://doi.org/10.1021/JS9601896.

Harrell, C.R., Djonov, V., Fellabaum, C., Volarevic, V., 2018. Risks of using sterilization by gamma radiation: the other side of the coin. Int. J. Med. Sci. 15, 274. https://doi.org/10.7150/IJMS.22644.

Hasanain, F., Guenther, K., Mullett, W.M., Craven, E., 2014. Gamma sterilization of pharmaceuticals—a review of the irradiation of excipients, active pharmaceutical ingredients, and final drug product formulations. PDA J. Pharm. Sci. Technol. 68, 113–137. https://doi.org/10.5731/PDAJPST.2014.00955.

Herczeg, C.K., Song, J., 2022. Sterilization of polymeric implants: challenges and opportunities. ACS Appl. Bio Mater. 5, 5077–5088. https://doi.org/10.1021/ACSABM.2C00793.

Hill, P.J., Wadman, S.H., Bishopp, S.D., Wermink, T., Wells, G.J., Lohr, T.L., Lockemeyer, J.R., Rebsdat, S., Mayer, D., 2025. Ethylene Oxide. Ullmann's Encyclopedia of Industrial Chemistry, pp. 1–30. https://doi.org/10.1002/14356007.A10_117.PUB2.

Houriet, C., Claassen, E., Mascolo, C., Jöhri, H., Brieva, A., Szmolka, S., Vincent-Bonnieu, S., Suliga, A., Heeb, R., Gantenbein, S., Lafont, U., Rohr, T., Masania, K., 2025. 3D printing of liquid crystal polymers for space applications. Adv. Mater. Technol. 10, 2400571. https://doi.org/10.1002/ADMT.202400571.

Hussong, D., 2010. Sterile products: Advances and challenges in formulation, manufacturing and regulatory aspects-A regulatory review perspective. AAPS Pharm.Sci.Tech. 11, 1482–1484. https://doi.org/10.1208/S12249-010-9503-Z/METRICS.

Igartua, M., Hernández, R.M., Rosas, J.E., Patarroyo, M.E., Pedraz, J.L., 2008. γ-Irradiation effects on biopharmaceutical properties of PLGA microspheres loaded with SPf66 synthetic vaccine. Euro. J. Pharmac. Biopharmac. 69, 519–526. https://doi.org/10.1016/J.EJPB.2007.12.014.

ISO 10993-7, 2008. - Biological evaluation of medical devices — Part 7: Ethylene oxide sterilization residuals [WWW Document]. n.d. URL. https://www.iso.org/standard/34213.html. accessed 1.29.26.

Jacobs, G.P., 2022. Irradiation of pharmaceuticals: A literature review. Rad. Phys. Chem. 190, 109795. https://doi.org/10.1016/J.RADPHYSCHEM.2021.109795.

Jamalzadeh, M., Ngendahimana, T., Sobkowicz, M.J., 2024. Correlating color with free radical concentration in irradiated poly(ethylene terephthalate). Polymer (Guildf) 312, 127656. https://doi.org/10.1016/J.POLYMER.2024.127656.

Kaiser, D., Bauer, A., Lemmerer, M., Maulide, N., 2018. Amide activation: an emerging tool for chemoselective synthesis. Chem. Soc. Rev. 47, 7899–7925. https://doi.org/10.1039/C8CS00335A.

Kane, M.P., Tsuji, K., 1983. Radiolytic degradation scheme for 60co-irradiated corticosteroids. J. Pharm. Sci. 72, 30–35. https://doi.org/10.1002/JPS.2600720108.

Kozyra, A., Mugheirbi, N.A., Paluch, K.J., Garbacz, G., Tajber, L., 2018. Phase diagrams of polymer-dispersed liquid crystal systems of itraconazole/component immiscibility induced by molecular anisotropy. Mol. Pharm. 15, 5192–5206. https://doi.org/10.1021/ACS.MOLPHARMACEUT.8B00724/ASSET/IMAGES/MEDIUM/MP-2018-007245_M008.GIF.

Krupianskaya, K., Croonenborghs, B., Gillet, A., Appeltans, B., Meyers, A., DeMent, A., Van den Mooter, G., Van Schepdael, A., Haghedooren, E., 2022. Sterilization of micronized indomethacin. Front. Anal. Sci. 2, 1028752. https://doi.org/10.3389/FRANS.2022.1028752/BIBTEX.

Lambert, B.J., Mendelson, T.A., Craven, M.D., 2011. Radiation and ethylene oxide terminal sterilization experiences with drug eluting stent products. AAPS Pharm.Sci. Tech. 12, 1116–1126. https://doi.org/10.1208/S12249-011-9644-8/FIGURES/7.

Leuner, C., Dressman, J., 2000. Improving drug solubility for oral delivery using solid dispersions. Eur. J. Pharmaceut. Biopharma. 50, 47–60. https://doi.org/10.1016/S0939-6411(00)00076-X.

Li, L.C., Parasrampuria, J., Bommireddi, A., Pec, E., Dudleston, A., Mayoral, J., 1998. Moist-heat sterilization and the chemical stability of heat-labile parenteral solutions. Drug Dev. Ind. Pharm. 24, 89–93. https://doi.org/10.3109/03639049809082357.

Li, Z., Zhao, P., Ling, Z., Zheng, Y., Qu, F., Chang, H., 2024. An ultraswelling microneedle device for facile and efficient drug loading and transdermal delivery. Adv. Healthc. Mater. 13, 2302406. https://doi.org/10.1002/ADHM.202302406.

Marcos Rios, D., Atrous, M.A., Belhaoues, A., Burillo, G., Navarro, R., Marcos-Fernández, Á., 2026. Effect of gamma radiation on the chemical structure and physical properties of poly(butylene adipate-co-terephthalate). Polymers (Basel) 18, 683. https://doi.org/10.3390/POLYM18060683/S1.

McCrudden, M.T.C., Alkilani, A.Z., Courtenay, A.J., McCrudden, C.M., McCloskey, B., Walker, C., Alshraiedeh, N., Lutton, R.E.M., Gilmore, B.F., Woolfson, A.D., Donnelly, R.F., 2015. Considerations in the sterile manufacture of polymeric microneedle arrays. Drug Deliv. Transl. Res. 5, 3–14. https://doi.org/10.1007/S13346-014-0211-1/FIGURES/4.

Mendes, G.C., Brandão, T.R.S., Silva, C.L.M., 2012. Ethylene oxide (EO) sterilization of healthcare products. Sterilisation of Biomaterials and Medical Devices 71–96. https://doi.org/10.1533/9780857096265.71.

Mendes, G.C.C., Brandão, T.R.S., Silva, C.L.M., 2007. Ethylene oxide sterilization of medical devices: a review. Am. J. Infect. Control 35, 574–581. https://doi.org/10.1016/J.AJIC.2006.10.014.

Milicevic, D., Trifunovic, S., Galovic, S., Suljovrujic, E., 2007. Thermal and crystallization behaviour of gamma irradiated PLLA. Radiation Phys. Chem. 76, 1376–1380. https://doi.org/10.1016/J.RADPHYSCHEM.2007.02.035.

Mohr, D., Wolff, M., Kissel, T., 1999. Gamma irradiation for terminal sterilization of 17β-estradiol loaded poly-(d,l-lactide-co-glycolide) microparticles. J.Controlled Release 61, 203–217. https://doi.org/10.1016/S0168-3659(99)00118-2.

Murthy, N.S., Khanna, Y.P., Signorelli, A.J., 1994. Crystallinities of poly (chlorotrifluoroethylene) and its copolymers by differential scanning calorimetry, X-ray diffraction, and density measurements. Polym. Eng. Sci. 34, 1254–1259. https://doi.org/10.1002/pen.760341605.

Naunton, M., Al Hadithy, A.F.Y., Brouwers, J.R.B.J., Archer, D.F., 2006. Estradiol gel: Review of the pharmacology, pharmacokinetics, efficacy, and safety in menopausal women. Menopause 13, 517–527. https://doi.org/10.1097/01.GME.0000191881.52175.8C.

Nguyen, H., Morgan, D.A.F., Forwood, M.R., 2006. Sterilization of Allograft Bone: is 25 kGy the Gold Standard for Gamma Irradiation? Cell Tissue Bank. 2 (8), 81–91. https://doi.org/10.1007/S10561-006-9019-7, 2006 8.

Ogrodowczyk, M., Marciniec, B., Hofman, M., Naskrent, M., Kierzkowska, A., 2011. Influence of e-beam irradiation on sulfamethoxazole in solid state. Anal. Sci. 27, 203–208. https://doi.org/10.2116/ANALSCI.27.203/METRICS.

Pérez Davila, S., González Rodríguez, L., Chiussi, S., Serra, J., González, P., 2021. How to sterilize polylactic acid based medical devices? Polymers 13, 2115. https://doi.org/10.3390/POLYM13132115, 2021Page13, 2115.

Ravikumar, K., Sridhar, B., Krishnan, H., 2007. Zolmitriptan, an anti-migraine drug. Acta Crystallogr. Sect. E Struct. Rep. https://doi.org/10.1107/S1600536807011439. Online 63.

Rediguieri, C.F., Sassonia, R.C., Dua, K., Kikuchi, I.S., de Jesus Andreoli Pinto, T., 2016. Impact of sterilization methods on electrospun scaffolds for tissue engineering. Eur. Polym. J. 82, 181–195. https://doi.org/10.1016/J.EURPOLYMJ.2016.07.016.

Repka, M.A., Shah, S., Lu, J., Maddineni, S., Morott, J., Patwardhan, K., Mohammed, N. N., 2012. Melt extrusion: process to product. Expert Opin. Drug Deliv. (9), 105–125. https://doi.org/10.1517/17425247.2012.642365.

Rutala, W.A., Weber, D.J., 2023. Sterilization of 20 billion medical devices by ethylene oxide (ETO): Consequences of ETO closures and alternative sterilization technologies/solutions. Am. J. Infect. Control 51, A82–A95. https://doi.org/10.1016/j.ajic.2023.01.020.

Sartawi, Z., Blackshields, C., Ariamanesh, A., Farag, F.F., Griffin, B., Crean, A., Devine, K., Elkhashab, M., Aldejohann, A.M., Kurzai, O., Faisal, W., 2023. Glass Microneedles: a case study for regulatory approval using a quality by design approach. Adv. Mater., 2305834 https://doi.org/10.1002/ADMA.202305834.

Sekulic, A., Migden, M.R., Oro, A.E., Dirix, L., Lewis, K.D., Hainsworth, J.D., Solomon, J. A., Yoo, S., Arron, S.T., Friedlander, P.A., Marmur, E., Rudin, C.M., Chang, A.L.S., Low, J.A., Mackey, H.M., Yauch, R.L., Graham, R.A., Reddy, J.C., Hauschild, A., 2012. Efficacy and Safety of Vismodegib in Advanced Basal-Cell Carcinoma. N. Engl. J. Med. 366, 2171. https://doi.org/10.1056/NEJMOA1113713.

Simmons, A., 2012. Future trends for the sterilisation of biomaterials and medical devices. Sterilisation of Biomaterials and Medical Devices 310–320. https://doi.org/10.1533/9780857096265.310.

Speleers, Q., Meyers, A., Rashid, H., Dubbelboer, Y., Vanneste, E., Croonenborghs, B., Gillet, A., DeMent, A., Van Schepdael, A., Haghedooren, E., 2025. On the stability of steroids upon gamma and e-beam irradiation and the protective effect of inert conditions. Molecules 30, 2605. https://doi.org/10.3390/MOLECULES30122605, 2025Page302605.

Spencer, C.M., Gunasekara, N.S., Hills, C., 1999. Zolmitriptan. a review of its use in migraine. Drugs 58, 347–374. https://doi.org/10.2165/00003495-199958020-00016/METRICS.

Swathi, H.P., Anusha Matadh, V., Paul Guin, J., Narasimha Murthy, S., Kanni, P., Varshney, L., Suresh, S., Shivakumar, H.N., 2020. Effect of gamma sterilization on the properties of microneedle array transdermal patch system. Drug Dev. Ind. Pharm. 46, 606–620. https://doi.org/10.1080/03639045.2020.1742144.

Tipnis, N.P., Burgess, D.J., 2018. Sterilization of implantable polymer-based medical devices: a review. Int. J. Pharm. 544, 455–460. https://doi.org/10.1016/J.IJPHARM.2017.12.003.

Tyski, S., Burza, M., Laudy, A.E., 2025. Microbiological contamination of medicinal products —is it a significant problem? Pharmaceuticals 18, 946. https://doi.org/10.3390/PH18070946, 2025Page18, 946.

Van Cauwenbergh, T., Theys, E., Stroeykens, D., Croonenborghs, B., Gillet, A., DeMent, A., Van Schepdael, A., Haghedooren, E., 2022. The effect of gamma and ethylene oxide sterilization on a selection of active pharmaceutical ingredients for Ophthalmics. J. Pharm. Sci. 111, 2011–2017. https://doi.org/10.1016/J.XPHS.2022.01.020.

Varshney, L., Dodke, P.B., 2004. Radiation effect studies on anticancer drugs, cyclophosphamide and doxorubicin for radiation sterilization. Rad. Phys. Chem. 71, 1103–1111. https://doi.org/10.1016/J.RADPHYSCHEM.2003.12.052.

Vranić, E., 2004. Amorphous pharmaceutical solids. Bosn. J. Basic Med. Sci. 4, 35. https://doi.org/10.17305/BJBMS.2004.3383.

WESTERBERG, D.P., VOYACK, M.J., 2013. Onychomycosis: current trends in diagnosis and treatment. Am. Fam. Physician 88, 762–770.

Yang, Y., Gao, Y., Mei, X., 2013. Effects of formulation parameters on encapsulation efficiency and release behavior of thienorphine loaded PLGA microspheres. Pharm. Dev. Technol. 18, 1169–1174. https://doi.org/10.3109/10837450.2011.618948.

Yu, L., 2001. Amorphous pharmaceutical solids: preparation, characterization and stabilization. Adv. Drug Deliv. Rev. 48, 27–42. https://doi.org/10.1016/S0169-409X(01)00098-9.